

Structural evolution and molecular dissociation of H2S under high pressures

Wen-Ji Shen(沈文吉)1, Tian-Xiao Liang(梁天笑)1, Zhao Liu(刘召)1, Xin Wang(王鑫)1,
De-Fang Duan(段德芳)1, Hong-Yu Yu(于洪雨)1,†, and Tian Cui(崔田)2,1,‡
Citation: Chin. Phys. B, 2022, 31 (7): 076102 DOI: 10.1088/1674-1056/ /ac5980
Journal homepage: http://cpb.iphy.ac.cn; http://iopscience.iop.org/cpb

What follows is a list of articles you may be interested in

Structural evolution and bandgap modulation of layered *β*-$GeSe_2$ single crystal under high pressure

Hengli Xie(谢恒立), Jiaxiang Wang(王家祥), Lingrui Wang(王玲瑞), Yong Yan(闫勇), Juan Guo(郭娟), Qilong Gao(高其龙), Mingju Chao(晁明举), Erjun Liang(梁二军), and Xiao Ren(任霄)
Chin. Phys. B, 2022, 31 (**7**): 076101. DOI: 10.1088/1674-1056/ac6db8

Raman spectroscopy investigation on the pressure-induced structural and magnetic phase transition in two-dimensional antiferromagnet $FePS_3$

Hong Zeng(曾鸿), Tingting Ye(叶婷婷), Peng Cheng(程鹏), Deyuan Yao(姚德元), and Junfeng Ding(丁俊峰)
Chin. Phys. B, 2022, 31 (**5**): 056109. DOI: 10.1088/1674-1056/ac5a41

Temperature dependence of bismuth structures under high pressure

Xiaobing Fan(范小兵), Shikai Xiang(向士凯), and Lingcang Cai(蔡灵仓)
Chin. Phys. B, 2022, 31 (**5**): 056101. DOI: 10.1088/1674-1056/ac398d

Dependence of nitrogen vacancy color centers on nitrogen concentration in synthetic diamond

Yong Li(李勇), Xiaozhou Chen(陈孝洲), Maowu Ran(冉茂武), Yanchao She(佘彦超), Zhengguo Xiao(肖政国), Meihua Hu(胡美华), Ying Wang(王应), and Jun An(安军)
Chin. Phys. B, 2022, 31 (**4**): 046107. DOI: 10.1088/1674-1056/ac3220

Pressure dependence of the thermal stability in $LiMn_2O_4$

Yan Zeng(曾彦), Hao Liang(梁浩), Shixue Guan(管诗雪), Junpu Wang(王俊普), Wenjia Liang(梁文嘉), Mengyang Huang(黄梦阳), and Fang Peng(彭放)
Chin. Phys. B, 2022, 31 (**1**): 016104. DOI: 10.1088/1674-1056/ac1932

Structural evolution and molecular dissociation of H_2S under high pressures

Wen-Ji Shen(沈文吉)[1], Tian-Xiao Liang(梁天笑)[1], Zhao Liu(刘召)[1], Xin Wang(王鑫)[1], De-Fang Duan(段德芳)[1], Hong-Yu Yu(于洪雨)[1,†], and Tian Cui(崔田)[2,1,‡]

[1] *College of Physics, Jilin University, Changchun* 130012, *China*
[2] *Institute of High Pressure Physics, School of Physical Science and Technology, Ningbo University, Ningbo* 315211, *China*

(Received 28 October 2021; revised manuscript received 30 January 2022; accepted manuscript online 2 March 2022)

Solid H_2S as the precursor for H_3S with incredible superconducting properties under high pressure, has recently attracted extensive attention. Here in this work, we propose two new phases of H_2S with $P4_2/n$ and $I4_1/a$ lattice symmetries in a pressure range of 0 GPa–30 GPa through first-principles structural searches, which complement the phase transition sequence. Further an *ab initio* molecular dynamics simulation confirms that the molecular phase $P2/c$ of H_2S is gradually dissociated with the pressure increasing and reconstructs into a new $P2_1/m$ structure at 160 GPa, exhibiting the superconductivity with T_c of 82.5 K. Our results may provide a guidance for the theoretical study of low-temperature superconducting phase of H_2S.

Keywords: high pressure, crystal structure, phase transition, superconductivity

PACS: 61.50.Ks, 82.33.Pt, 74.25.–q **DOI:** 10.1088/1674-1056/ac5980

1. Introduction

In previous work, Ashcroft[1,2] made two predictions based on BCS theory: metallic hydrogen is most likely a room temperature superconductor and hydrogen-dominated metallic alloys are potential high temperature superconductors at high pressure. However, the realization of metal hydrogen requires extremely high pressure, and a controversial high-pressure experiment shows that it needs at least 495 GPa.[3] Based on the introduction of non-hydrogen elements to stimulate chemical precompression, the metallization pressure of hydrogen-rich compounds is low,[4–9] like 40 GPa at room temperature for hydride phosphine,[10–12] which is much lower than 495 GPa for metallic hydrogen. In 2014, Duan *et al.* predicted the existence of *Im*-3*m*_H_3S[13] and put forward that H_3S has a high superconducting transition temperature (T_c) higher than 190 K at 200 GPa. In 2015, Drozdov *et al.* experimentally reported a high temperature superconductor with T_c of 203 K by compressing solid H_2S.[14] Then, a series of experimental and theoretical researches confirmed the high T_c of 203 K derived from the theoretically proposed *R*3*m* or *Im*-3*m*_H_3S.[15–20] Further researches are needed on the decomposition products of H_2S under high pressure, and on the role played by the decomposition products in forming H_3S.

The H_2S has a simple structure at low pressure, but leads a series of complex phase transition process under different pressures and temperatures. When the temperature drops gradually under ambient pressure, a phase transition of fluid phase → phase I (*Fm*-3*m*)[21] → phase II (*Pa*-3)[21] → phase III (*Pbcm*) happens to H_2S.[21] *Ab initio* calculation showed that at 0 K, the phase III (*Pbcm*) transforms into the $P2/c$ at 8.7 GPa → the *Pc* at 29 GPa → the $Pmc2_1$ at 65 GPa → the *P*-1 at 80 GPa → the *Cmca* at 160 GPa.[22] If pressure increased at room temperature, another phase transition process would occur, which is fluid phase → phase I → phase I′ ($P2_13$).[23] → phase IV′ (*Ibca*)[24–26] → phase IV,[23] and H_2S would finally be decomposed at 27 GPa and turn into the mixture of S, H_2 and phase V.[27,28] The infrared spectra at high pressure and room temperature also revealed that the molecular dissociation of molecular H_2S occurs under nearly 46 GPa, and metallization of molecular H_2S occurs near 96 GPa, respectively.[29] On the other hand, the phase transition process was phase III → phase III′ (*Pcca*)[23] → phase IV′ → phase IV with pressurization at 100 K. Combined with the experiments and calculations, the phase diagram of H_2S has also been gradually filled,[23,30] and several energetically competitive stoichiometries other than H_2S and H_3S have been proposed, which are HS_2, H_2S_3, H_3S_2, H_3S_5, H_4S_3, and H_5S_8.[31,32] The temperature had a key influence on the crystal structure, phase transition pressure, decomposition products, and decomposition path of H_2S.[28,33] We have performed MD simulations on experimental conditions by choosing different initial structures, and obtained different simulation results.[34–36] And the phase IV ($P2/c$) predicted theoretically is in good agreement with experimental result, and is appropriate to be selected as an initial structure. Accordingly, it is necessary to adopt finite temperature molecular dynamics to study the molecular dissociation process.

In our work, we explore the phase transition of H_2S via

†Corresponding author. E-mail: yuhongyu@jlu.edu.cn
‡Corresponding author. E-mail: cuitian@jlu.edu.cn

© 2022 Chinese Physical Society and IOP Publishing Ltd

ab initio structure searching and *ab initio* molecular dynamics (AIMD) to complement its important phase transition sequence. Three new structures of H–S compounds are discovered for the first time, and the relevant thermodynamic properties and the superconductivity properties are revealed. Remarkably, we also investigate the dissociation process of H_2S at high pressure, and our calculation results can help to further clarify the phase diagrams of H_2S at higher pressures and temperatures.

2. Computational details

Structure of H_2S were investigated with *ab initio* calculations as implemented in the Universal Structure Predictor: Evolutionary Xtallography (USPEX)[37–39] in a pressure range of 0 GPa–30 GPa in pressure steps of 5 GPa. The Vienna *ab initio* simulation packages (VASP) code[40] was used to optimize crystal structures and calculate the electronic properties, where the Perdew–Burke–Ernzerhof (PBE)[41] of generalized gradient approximation (GGA)[42] was chosen and used as an exchange–correlation functional. And the projector-augmented wave method (PAW)[43] potentials with the $1s^1$ and $3s^23p^4$ configurations treated as valence electrons for H and S were used. Kinetic cutoff energy of 400 eV was selected and Monkhorst–Pack k-mesh with grid spacing of $2\pi \times 0.03$ Å^{-1} was then adopted to ensure that the enthalpy converges to less than 1 meV/atom. The calculations on phonons were carried out by the PHONOPY code,[44] which showed good agreement with those computed using the Quantum-ESPRESSO (QE) code.[45] Electron phonon coupling (EPC) matrix elements were calculated using density functional perturbation theory as implemented in the Quantum ESPRESSO package. Ultra-soft pseudopotential[46] was used with an 80 Ry (1 Ry = 13.6056923(12) eV) kinetic energy cutoff and an 800-Ry charge density cutoff. A $12 \times 12 \times 20$ k-mesh grid was used for Brillouin zone (BZ) integration in electronic calculations, and EPC matrix elements were calculated in $3 \times 3 \times 5$ q-points grid. Electronic smearing in self-consistent calculation adopted Methfessel–Paxton first-order spreading[47] with a smearing width of 0.025 Ry. Furthermore, we also performed extensive *ab initio* molecular dynamics (AIMD) simulations based on the Born–Oppenheimer approximation implemented in VASP, and set the temperature range to be from 100 K to 250 K. The AIMD simulation for H_2S phases were performed in $2 \times 2 \times 2$ supercells (384 atoms) for $P4_2/n$ and $I4_1/a$, $2 \times 2 \times 3$ supercells (144 atoms) for $P2/c$, and $2 \times 3 \times 3$ supercells (108 atoms) for P-1 with $2 \times 2 \times 2$ k-mesh. We adopted the *NPT* (N-constant is the number of particles, P-constant is the pressure, and T-constant is the temperature) ensemble, lasting for 12 ps in time steps of 1 fs, and we allowed 2-ps thermalization and then extracted data from the last 10 ps.

3. Results and discussion

Here, the global structural evolution algorithm variable-composition predictions are realized in over 2×10^4 structures, and 2, 4, 6, 8, and 16 H_2S formula units are employed in a pressure range from 0 GPa to 30 GPa. Two new phases of H_2S with space groups of $P4_2/n$ and $I4_1/a$ are uncovered as shown in Fig. 1. The H atoms occupy 8f sites, and S atoms 8f sites in the $P4_2/n$ lattice. And H atoms account for 16f sites, and S atoms 16f sites in the $I4_1/a$ lattice, as shown in Table S1 in the Supplementary materials (SM). As shown in Figs. 1(a) and 1(b), $P4_2/n$ and $I4_1/a$crystal lattice contain isolated H_2S units inside, and we can observe from the structure intuitively that $P4_2/n$ and $I4_1/a$ are molecular crystals. The enthalpies of two new structures together with the ambient-pressure *Pbcm* (phase III) and another four low-enthalpy structures mentioned by Li *et al.*[22] are plotted as a function of pressure in Fig. 2. With pressure increasing, *Pbcm* (phase III) of H_2S crystallize into a $P4_2/n$ phase at about 3 GPa. Above 10 GPa, $P4_2/n$ phase turns into $P2/c$ phase,[22] and then transforms into $I4_1/a$ at about 20 GPa.

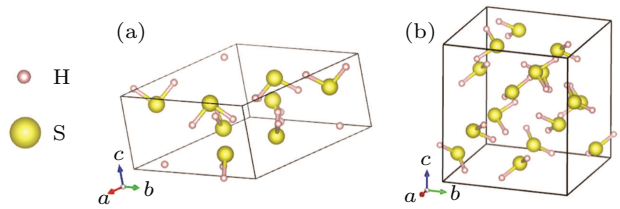


Fig. 1. Predicted energetically stable crystal structures of (a) $P4_2/n$ and (b) $I4_1/a$ in structural evolution.

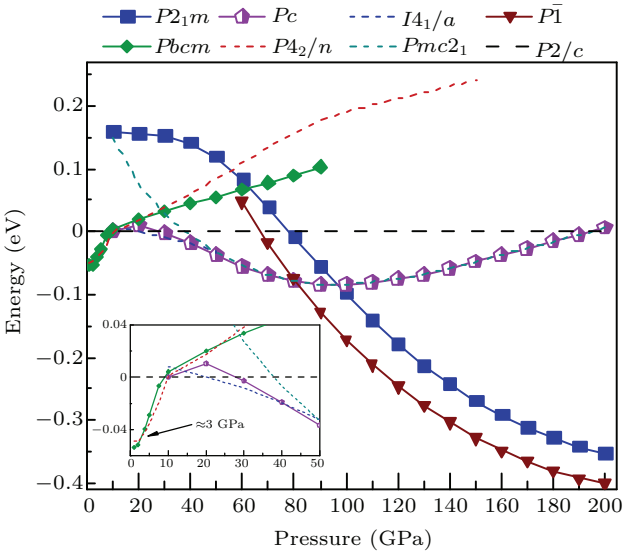


Fig. 2. Curves of calculated enthalpy *versus* pressure for phases $P2_1m$, $P4_2/n$, $I4_1/a$, *Pbcm* (phase III),[21] P-1,[22] $Pmc2_1$,[22] and Pc[22] relative to $P2/c$.[22]

Phonon dispersion calculations of $P4_2/n$ and $I4_1/a$ structures in Figs. 3(a) and 3(b) do not give any imaginary frequencies. Therefore, $P4_2/n$ and $I4_1/a$ are dynamically stable at corresponding pressure points. The electronic band structures of H_2S are calculated at 10 GPa for $P4_2/n$ phase and at 30 GPa for $I4_1/a$ phase as shown in Figs. 3(c) and 3(d). The results

of electrical properties show that the new phases are insulators because band gaps between valence band and conduction band are quite large, specifically, 3.3 eV for $P4_2/n$ and 2.5 eV for $I4_1/a$. The p-electrons of S dominate the density of states nearby the fermi surface for both $P4_2/n$ and $I4_1/a$, and dominates the density of states of valence bands significantly.

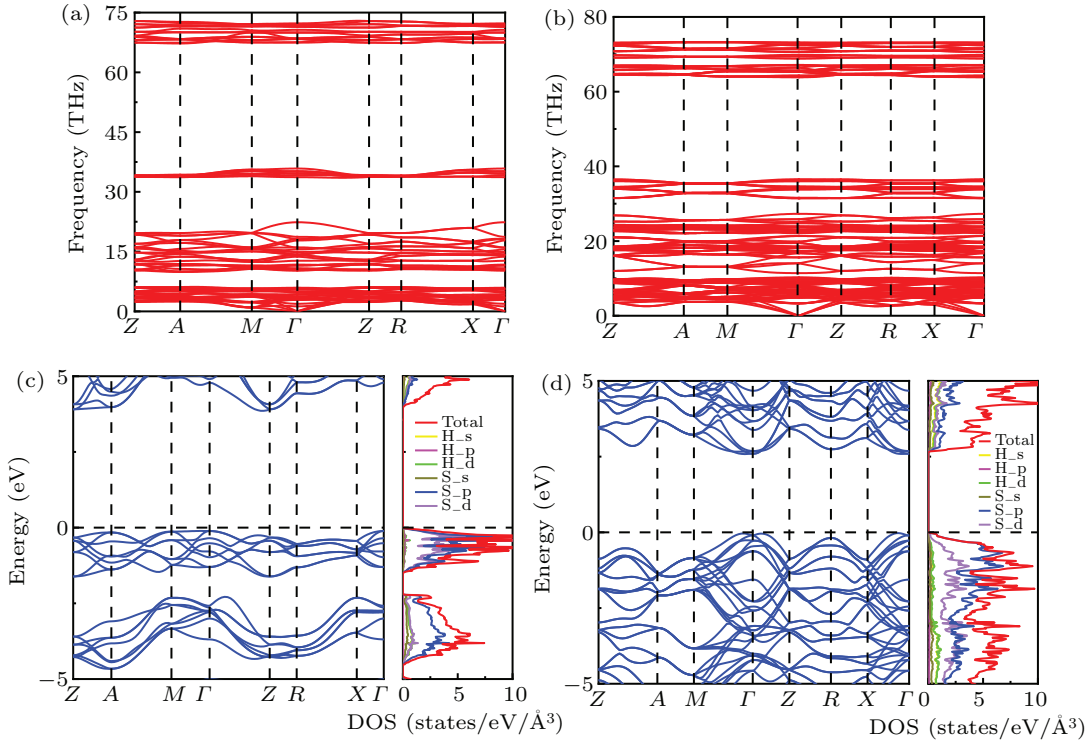


Fig. 3. Calculated phonon dispersion curves for (a) $P4_2/n$ at 10 GPa and (b) $I4_1/a$ at 30 GPa, and corresponding electronic band structure and projected density of states for (c) $P4_2/n$ at 10 GPa and (d) $I4_1/a$ at 30 GPa.

To further study the dynamical properties of phases $P4_2/n$ and $I4_1/a$, *ab initio* molecular dynamics (AIMD) simulations within finite temperature are performed. By calculating the radial distribution function (RDF) g_{SH} of the averaged S-H positions, we find that crystals of $P4_2/n$ and $I4_1/a$ do not change obviously with temperature rising (see Figs. S1(d)–S1(f) and Figs. S2(d)–S2(f) in the SM). To sum up the results discussed above, the final phase transition sequence at zero temperature is *Pbcm* (phase III) $\rightarrow P4_2/n \rightarrow P2/c \rightarrow I4_1/a \rightarrow$ *Pc* below 30 GPa.

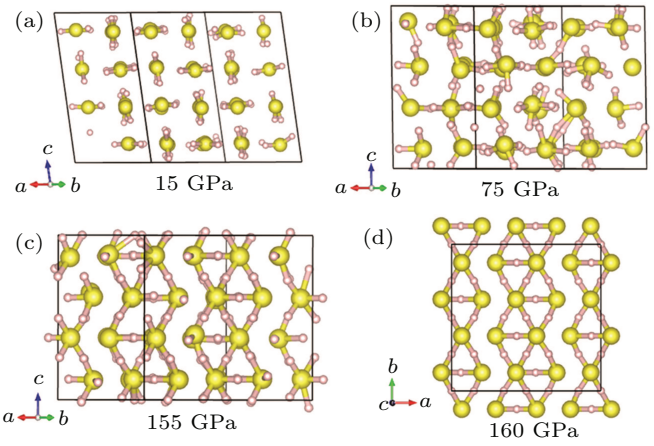


Fig. 4. Snapshot of MD trajectory at 250 K and (a) 15 GPa, (b) 75 GPa, and (c)155 GPa. (d) New $P2_1/m$ phase of H_2S.

Considering the energetically favored candidate for phase IV is the $P2/c$, whose x-ray diffraction patterns can reproduce the main peaks of phase IV below 2θ of 20°, as well as the weak peaks around 25°. We perform the AIMD simulations in $2 \times 2 \times 3$ supercells for $P2/c$-H_2S at 100, 200, and 250 K in a pressure range of 15 GPa–175 GPa to study the molecular dissociation and superconducting phase of H_2S. By observing the snapshots of MD trajectory at 250 K (See Figs. 4(a)–4(c)), we can clearly observe the dissociation process of $P2/c$-H_2S and the reconstruction process of a new polymeric structure. By statistically averaging the trajectories of S and H atoms at 155 GPa and 250 K, we obtain the symmetry and atomic coordinates of this new structure (see Table 1).

To further examine the dissociation and reconstruction process of H_2S, the values of RDF g_{SH} are obtained from the AIMD simulations at 250 K and different pressures, and the results are shown in Fig. 5. When the pressure increases up to 45 GPa, the first peak of g_{SH} remains almost unchanged but the second peak shifts left forward obviously for each curve. With the snapshots of MD trajectory, we can see that the H_2S keeps $P2/c$ symmetry but the distances between S and H atoms in different H_2S molecules keep closer to each other as the pressure increases. From 55 GPa to 95 GPa, the first peak shifts slightly from 1.36 Å to 1.37 Å, and the first peak and the second peak tend to merge together (see Fig. 5 and Fig. S3 in the SM). It is due to the nearest S and H atoms in different H_2S molecules get closer enough and the interactions between

these S and H atoms get stronger. As the pressure increases, some protons occupy two symmetric positions along the S–S bond with equal probability gradually, just like the process of symmetric hydrogen bond of ice phase VII,[48] meanwhile some H_2S molecules start to decompose into HS+H_3S. At even higher pressure, we can see a shoulder clearly in the g_{SH} at 115 GPa, indicating that H_2S molecules start to be reconstructed. Especially when pressure increases from 115 GPa to 135 GPa, the bond length of H–S gradually increases to 1.43 Å, forming a new structure.

Table 1. Predicted structural parameters of H_2S_$P2_1/m$.

Compounds	Space groups	Lattice parameters	Atomic coordinates (fractional)	
			Atoms	(X,Y,Z)
H_2S	$P2_1/m$	$a=4.433$ Å	H (4f)	(0.700, 0.002, 0.134)
(160 GPa)	(Phase IV)	$b=4.434$ Å	H (2c)	(0.0, 0.0, 0.500)
		$c=2.619$ Å	H (2e)	(0.127, 0.250, 0.164)
		$\alpha=\gamma=90$ (°)	S (2e)	(0.863, 0.250, 0.838)

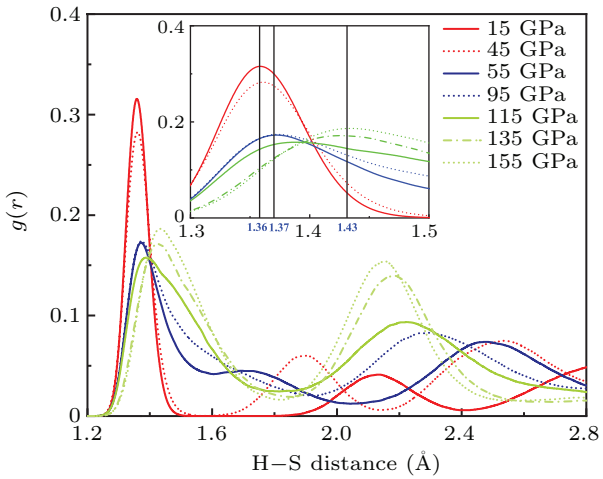


Fig. 5. RDFs of averaged S–H positions under different pressures of H_2S–$P2c$ at 250 K.

In the same pressure interval, combining the g_{SH} and AIMD snapshots of $P2/c$ phase at 100 K and 200 K, we can see that the symmetric hydrogen bonds appear at 75 GPa and 85 GPa, respectively. More seriously, at 100 K and 200 K (see Figs. S4 and S5 in the SM), although partial H_2S molecules are dissociated at higher pressure, the reconstruction is not obvious until 155 GPa. In conclusion, the AIMD results indicate that the new $P2_1/m$ structure of H_2S can be derived from dissociation of $P2/c$ phase, indicating the superconductivity at 160 GPa. In our further investigation, the superconducting transition temperature T_C for $P2_1/m$ at 160 GPa was estimated through the McMillan equation:

$$T_c = \frac{\omega_{log}}{1.2}\exp\left[\frac{-1.04(1+\lambda)}{\lambda-\mu^*-0.62\lambda\mu^*}\right], \tag{1}$$

where λ is the EPC constant, ω_{log} is an appropriately defined logarithmic average frequency, μ^* is the Coulomb pseudopotential, which is a parameter accounting for the effective Coulomb repulsionn generally takes $\mu^*=0.1$ for hydride, λ is the EPC parameter, and logarithmic average frequency ω_{log} is the logarithmic average frequency: λ and ω_{log} are calculated from

$$\lambda = \int_0^{\omega_{max}} \frac{2\alpha^2F(\omega)}{\omega}d\omega, \tag{2}$$

$$\omega_{log} = \exp\left(\frac{2}{\lambda}\int_0^{\omega_{max}} \frac{2\alpha^2F(\omega)\ln\omega}{\omega}d\omega\right). \tag{3}$$

The superconducting transition temperature T_C for $P2_1/m$ is estimatedat 82.5 K under 160 GPa, obtaining $\lambda=1.93$ and $\omega_{log}=588.1$ K correspondingly.

As shown in Fig. 2, at 80 GPa–160 GPa, P-1 phase is more energetically stable than others. Hence, we also perform the AIMD simulations in $2\times3\times3$ supercells for P-1-H_2S at 100 K, 200 K, and 250 K in a pressure range of 90 GPa–200 GPa. The P-1 phase will finally turn into the *Cmca* phase[22] with pressure increasing. From the snapshots of MD trajectory at 250 K (see Figs. 6(a)–6(c)), we can see that the P-1 phase remains stable in a pressure range of 90 GPa–120 GPa. The P-1 phase contains the H_3S–SH_3 units which are connected mutually through planar symmetric hydrogen bonds of two H atoms. Under further compression, the P-1 phase eventually transforms into the *Cmca* phase, and each S atom in the *Cmca* structure bonds with two H atoms in adjacent two layers, and all H atoms bond with two S atoms, which fits well with our simulations.

Furthermore, the RDF g_{SH}, are also obtained from the AIMD simulations at 100 K, 200 K, and 250 K, and the results are shown in Fig. 7. With pressure increasing at 250 K, the first peak at 1.4 Å and the second peak at 1.9 Å simultaneously shift rightward and leftward,for each curve, respectively. When the pressure increases to 140 GPa, the second peak becomes a shoulder at about 1.7 Å and completely merge together with the first peak above 160 GPa. This is similar to the dissociation and reconstruction process of $P2/c$, and the same results are obtained at 200 K and 100 K (see Figs. 6(d) and 6(e)). And as the temperature decreases, the pressure of the phase transition from P-1 to *Cmca* increases. With the RDF g_{SH}, as shown in Fig. 7, we can see that the transition pressure at 250 K, 200 K, and 100 K are about 140 GPa, 160 GPa, and 180 GPa, respectively.

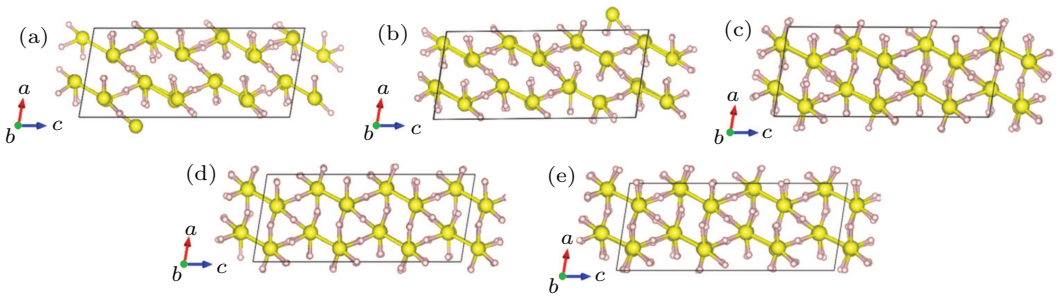


Fig. 6. Snapshot of MD trajectory at (a) 90 GPa and 250 K, (b) 120 GPa and 250 K, (c) 160 GPa and 250 K, (d) 180 GPa and 100 K, and (e) 180 GPa and 200 K.

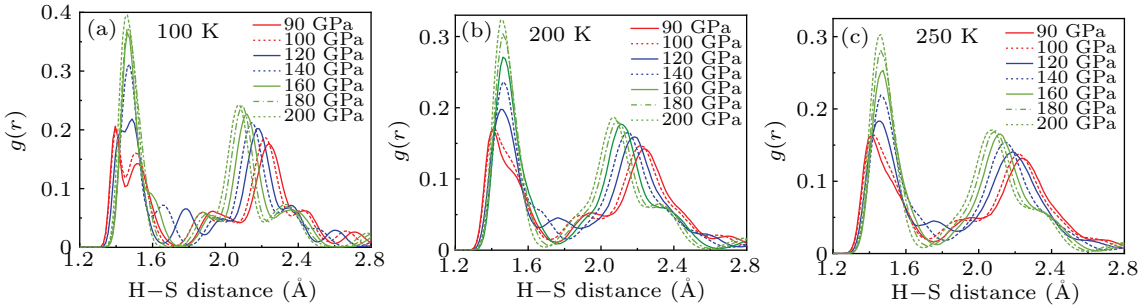


Fig. 7. Dynamical behaviors of H and S atoms in S–H compounds, obtained from AIMD simulations for *P*-1 phase in solid states, for RDFs of averaged S–H positions at (a) 100 K, (b) 200 K, and (c) 250 K.

4. Conclusions

In this work, we predict two new structures of H_2S with $P4_2/n$ and $I4_1/a$ in a lower pressure range (0 GPa–30 GPa). The $P4_2/n$ phase and the $I4_1/a$ phase are dynamically stable and insulators. The final phase transition sequence at zero temperature and high pressure is from *Pbcm* (phase III) to $P4_2/n$ at 3 GPa, to $P2/c$ (phase IV) at 10 GPa, then to $I4_1/a$ at 20 GPa, and finally to *Pc* at 40 GPa. Our calculations for thermodynamic, electronic, and dynamic properties reveal this newly discovered phase transition. We also preform the AIMD simulation for $P2/c$ of H_2S in different pressure and temperature ranges. At 250 K, the radial distribution function calculations obviously show the symmetric hydrogen bond and the reconstruction of H_2S as the pressure increases. Besides, we find a new $P2_1/m$ phase at 160 GPa and 250 K. The $P2_1/m$ phase may be a potential superconductor with T_C of 82.5 K at 160 GPa. This study may be helpful in studying the low-temperature superconducting phase of H_2S. And this result may be conducive to further clarifying the phase diagram of H_2S and other H–S compounds under higher pressure and temperature.

Acknowledgements

The computation of this work was carried out at the High-Performance Computing Center (HPCC) of Jilin University, Beijing Super Cloud Computing Center, and TianHe-1(A) at the National Supercomputer Center in Tianjin.

Project supported by the National Natural Science Foundation of China (Grant Nos. 11704143, 11804113, 11604023, and 12122405).

References

[1] Ashcroft N W 1968 *Phys. Rev. Lett.* **21** 1748
[2] Ashcroft N W 2004 *Phys. Rev. Lett.* **92** 187002
[3] Dias R P and Silvera I F 2017 *Science* **355** 715
[4] Zhou D, Jin X, Meng X, Bao G, Ma Y, Liu B and Cui T 2012 *Phys. Rev. B.* **86** 014118
[5] Song H, Zhang Z, Cui T, Pickard C J, Kresin V Z and Duan D 2021 *Chin. Phys. Lett.* **38** 107401
[6] Tian C, Huang X, Huang Y, Li X, Zhou D, Wang X and Cui T 2019 *Chin. Phys. Lett.* **36** 106101
[7] Zhou X, Oganov A R, Dong X, Zhang L, Tian Y and Wang H 2011 *Phys. Rev. B* **84** 054543
[8] Liu M, Duan D, Huang Y, Liang Y, Huang X and Cui T 2019 *Chin. Phys. Lett.* **36** 086401
[9] Gao, G, Wang L, Li M, Zhang J, Howie R T, Gregoryanz E, Struzhkin V V, Wang L and Tse J S 2021 *Mater. Today Phys.* **21** 100546
[10] Wang H, Li X, Gao G, Li Y and Ma Y 2018 *Wires. Comput. Mol.* **8** e1330
[11] Liu H, Li Y, Gao G, Tse J S and Naumov I I 2016 *J. Chem. Phys. C* **120** 3458
[12] Drozdov A, Eremets M and Troyan I 2015 arXiv:1508.06224 [cond-mat.supr-con]
[13] Duan D, Liu Y, Tian, F, Li D, Huang X, Zhao Z, Yu H, Liu B, Tian W and Cui T 2014 *Sci. Rep.* **4** 6968
[14] Drozdov A P, Eremets M I, Troyan I A, Ksenofontov V and Shylin S I 2015 *Nature* **525** 73
[15] Capitani F, Langerome B, Brubach J B, Roy P, Drozdov A, Eremets M I, Nicol E J, Carbotte J P and Timusk T 2017 *Nat. Phys.* **13** 859
[16] Duan D, Huang X, Tian F, Li D, Yu H, Liu Y, Ma Y, Liu B and Cui T 2015 *Phys. Rev. B* **91** 180502
[17] Einaga M, Sakata M, Ishikawa T, Shimizu K, Eremets M I, Drozdov A P, Troyan I A, Hirao N and Ohishi Y 2016 *Nat. Phys.* **12** 835
[18] Goncharov A F, Lobanov S S, Prakapenka V B and Greenberg E 2017 *Phys. Rev. B* **95** 140101
[19] Quan Y and Pickett W E 2016 *Phys. Rev. B* **93** 104526
[20] Sano W, Koretsune T, Tadano T, Akashi R and Arita R 2016 *Phys. Rev. B* **93** 094525
[21] Cockcroft J K and Fitch A N 1990 *Z. Kristallogr.* **193** 1

[22] Li Y, Hao J, Liu H, Li Y and Ma Y 2014 *J. Chem. Phys.* **140** 174712

[23] Fujihisa H, Yamawaki H, Sakashita M and Aoki K 1998 *Phys. Rev. B* **57** 2651

[24] Fujihisa H, Yamawaki H, Sakashita M, Nakayama A, Yamada T and Aoki K 2004 *Phys. Rev. B* **69** 214102

[25] Wang L, Tian F, Feng W, Chen C, He Z, Ma Y, Cui T, Liu B and Zou G 2010 *J. Chem. Phys.* **132** 164506

[26] Wang L, He Z, Ma Y, Cui T, Liu B and Zou G 2007 *J. Phys.: Condens. Matter* **19** 425232

[27] Shimizu H, Nakamichi Y and Sasaki S 1991 *J. Chem. Phys.* **95** 2036

[28] Rousseau R, Boero M, Bernasconi M, Parrinello M and Terakura K 2000 *Phys. Rev. Lett.* **85** 1254

[29] Sakashita M, Yamawaki H, Fujihisa H, Aoki K, Sasaki S and Shimizu H 1997 *Phys. Rev. Lett.* **79** 1082

[30] Duwal S and Yoo C S 2016 *J. Phys. Chem. C* **120** 21770

[31] Goncharov A F, Lobanov S S, Kruglov I, Zhao X, Chen X, Oganov A R and Prakapenka V B 2016 *Phys. Rev. B* **93** 174105

[32] Li Y, Wang L, Liu H, Zhang Y, Hao J, Pickard C J, Nelson J R, Needs R J, Li W, Huang Y, Errea I, Calandra M, Mauri F and Ma Y 2016 *Phys. Rev. B* **93** 020103

[33] Huang X, Wang X, Duan D, Sundqvist B, Li X, Huang Y, Yu H, Li F, Zhou Q, Liu B and Cui T 2019 *Nat. Sci. Rev.* **6** 713

[34] Majumdar A, Tse J S and Yao Y 2019 *Sci. Rep.* **9** 5023

[35] Majumdar A, Tse J S and Yao Y 2017 *Angew. Chem.* **129** 11548

[36] Yao Y and Tse J S 2018 *Chem. Eur. J.* **24** 1769

[37] Oganov A R and Glass C W 2006 *J. Chem. Phys.* **124** 244704

[38] Oganov A R, Lyakhov A O and Valle M 2011 *Acc. Chem. Res.* **44** 227

[39] Lyakhov A O, Oganov A R, Stokes H T and Zhu Q 2013 *Comput. Phys. Commun.* **184** 1172

[40] Kresse G and Furthmüller J 1996 *Comput. Mater. Sci.* **6** 15

[41] Perdew J P, Burke K and Ernzerhof M 1996 *Phys. Rev. Lett.* **77** 3865

[42] Perdew J P and Wang Y 1992 *Phys. Rev. B* **46** 12947

[43] Blöchl P E 1994 *Phys. Rev. B* **50** 17953

[44] Togo A, Oba F and Tanaka I 2008 *Phys. Rev. B* **78** 134106

[45] Giannozzi P, Baroni S and Bonini N, *et al.* 2009 *J. Phys.: Condens. Matter.* **21** 395502

[46] Baroni S, Gironcoli S and Corso A D 2001 *Rev. Mod. Phys.* **73** 515

[47] Vanderbilt D 1990 *Phy. Rev. B* **41** 7892

[48] Bernasconi M, Silvestrelli P and Parrinello M 1998 *Phys. Rev. Lett.* **81** 1235